International Journal of Current Engineering and Technology
ISSN 2277 - 4106

Available at http://inpressco.com/category/ijcet

Research Article

Performance Analysis of Single Slope Solar Stills at Different Inclination Angles: an Indoor Simulation

Nikhil Singh[a*]

[a]Department of Mechanical Engineering, SHIATS-DU, Allahabad-211007 (India)

Accepted 15 June 2013, Available online 19 June 2013, **Vol.3, No.2 (June 2013)**

Abstract

In this study, the performance of single slope solar stills inclined at 15^0, 30^0 & 45^0 have been investigated and compared to Dunkle model. It is found that the performance of present model is higher than that of Dunkle model. For the purpose of experiment constant temperature water bath has been used to maintain the steady state of water temperatures ranging from 40^o C to 70^o C. The yield obtained at an interval of every 30 minutes has been used to determine the values of constants C and n and consequently the performance parameters, internal heat transfer coefficients and internal mass transfer. The maximum internal mass transfer is obtained for condensing cover with inclination angle of 45^0 and the minimum for condensing cover with inclination angle of 15^0. The maximum and minimum percentage deviation in yield between the theoretical and practical values for condensing cover with inclination of 45° is -10.52% for 70° C & -1.96% for 45° C respectively.

Key words: *Solar Distillation, internal heat and mass transfer, inclination angle, condensing cover*

1. Introduction

The water and the energy can be considered as the two most essential things for sustaining life, and both are to be conserved and preserved for the sustainable development of the world. There is a severe crisis of energy and water in the world today, especially in the 3rd world countries. Over 97% of water available on the earth's surface is salty, approximately 2% of the water in the world at present is stored as ice in polar region, and 1% water is available in rivers, lakes and underground reservoirs. This 1% water has also been degraded by environmental pollution caused predominantly by anthropogenic activities. The problem of chemical contamination is also prevalent. The major chemical parameters of concern are fluoride and arsenic. Iron is also emerging as a major problem with many habitations showing excess iron in the water samples. This has led to the intensification of the drinking water crisis in the world.

Water desalination is an appropriate technique to meet the water demand in many countries of the world. In this technique the salt is separated from the water by the process of evaporation and then the separated vapours are condensed to obtain desalinated water. Though the technique is effective but it requires energy to cause evaporation. As fossil fuel resources are depleting with each passing day we cannot depend on them for prolonged period. There is therefore the need to explore a sustainable, green and cheap source of energy. Of lately solar energy is being seen as sustainable, green and cheap energy and solar desalination is gaining more importance for obtaining potable water.

The main advantage of this process is that, it does not utilize costly conventional fossil fuels, which create the problem and also the solar energy is abundantly and freely available.

2. Literature survey

The functional temperature range of solar driven distillation units is from 60^0 to 120^0 (Nafey A.S. *et al*, 2000) and the prediction of their performance mainly depends on accurate estimation of internal heat and mass transfer relations. E. Delyannis, (Delyannis E., 2003) carried out a historical review on desalination techniques and renewable energy utilization with an emphasis on solar energy utilization for desalination and concluded that what is a new development for us will be a history for next generation. **K.** Sampathkumar **(**Sampathkumar K. *et al*, 2010) carried out the detailed review of various designs of active solar stills and highlighted on various parameters affecting the performance of these solar stills. They carried out thermal modelling for various types of active single slope solar distillation system and highlighted on the scope for further areas of research. Many experimental and theoretical works have been conducted on single basin solar stills for testing the performance of different enhancement parameters. The oldest semi-empirical heat

*Corresponding author **Nikhil Singh** is working as Asst. Prof

and mass transfer relation for solar stills was given by Dunkle (Dunkle R.V., 1961). However, the relation developed by Dunkle has the following limitations:
a) It is valid for a low operating temperature range (45-500C).
b) It is independent of the cavity volume, i.e. the average spacing between the condensing and evaporative surfaces.
c) It is valid for cavities that have parallel condensing and evaporative surfaces.

Numerous empirical relations were formulated later on to predict the hourly and daily distillate output for different designs of solar distillation units. Most of these relations are based on simulation studies. Kumar et al (Kumar *et al,* 1996) has conducted thermal and computer modelling for finding the values of constants C and n and consequently heat and mass transfer coefficients for different types of solar still. (Lof G.O.G *et al,* 1961) have analysed heat and mass transfer of solar still in detail and studied the effect of various design parameters and climatic variables on the performance of a solar still. Numerical solution of the heat balance equations was then obtained with the aid of a digital computer. Sharma et al (Sharma V.B. *et al,* 1991) developed a method for estimation of heat transfer coefficients for upward heat flow and evaporation in still and calculation of hourly output was done with this new approach. It was observed that the performance of solar still has an agreement with the result of an analysis based on Dunkle's relation with a factor of 0.65 to account for instauration. Shukla et al (Shukla *et al,* 2005) has recently developed a model, based on regression analysis, to determine the values of constants C and n using the experimental data obtained from the stills. This method uses both inner and outer glass cover temperatures to determine the expressions for internal heat transfer coefficient and does not impose any limitations. (Aboul Enein S *et al,* 1998) presented a simple transient mathematical model for a single basin still through an analytical solution of the energy-balance equations for different parts of the still. The authors also investigated the thermal performance of the still both experimentally and theoretically, and the influence of cover slope on the daily productivity of the still. This transient mathematical model was used by (Akash B.A. *et al,* 1998) for a vertical solar still to conduct parametric investigation. He found that the daily productivity of the still increases with the increase of the still length, width, and wind speed up to typical values. (Akash B.A. *et al,* 2000) examined the effect of using a solar still with various cover tilt angles of 15, 25, 35, 45 and 55 º in outdoor conditions and the optimum tilt angle for water production was found to be 35º.

3. Experimental setup

The experimental set-up includes a constant temperature water bath, condensing covers inclined at 15°, 30° & 45°, digital temperature indicators, well calibrated thermocouples (by Zeal Thermometer), two transparent pipes of small diameter and a measuring flask. The output from the still is collected through a channel. Two plastic pipes are connected to this channel to drain the distilled water to an external measuring jar. The total capacity of the constant temperature bath is 40 L, and its effective evaporative surface area is 0.3 m × 0.4 m. The water is heated by bath heating coils. Table 1, shows the detailed dimensions of condensing covers and Fig. 1 shows the picture of fabricated condensing cover.

Table 1: detailed demensions of condensing covers

S. No	Parameter	Dimension of 15° (mm)	Dimensions of 30° (mm)	Dimensions of 45° (mm)
1	Length	430	430	430
2	Width	330	330	330
3	Higher height	300	440	625
4	Lower height	64	69	75

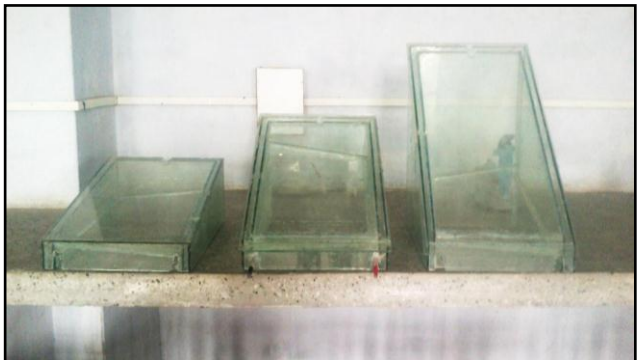

Figure 1: condensing covers

Condensing covers at three different inclination angles were fabricated in the lab with the help of common glass to make top inclined covers and 3 mm thick GRP (Glass Reinforced Plastic) sheets to make the side walls of the condensing covers. This glass reinforced plastic is manufactured by sticking many layers of corrugated sheets with special chemicals in such a manner that air is entrapped between its corrugated cavities, which provide a high degree of insulation for heat flow, which is a highly desired quality for the solar still material.

3.1 Procedure of Experiments

The experiments were conducted on different days in the month of June, 2012, on the campus of Sam Higginbottom Institute of Agriculture, Technology and sciences-Deemed to be University. The inclination angles of fabricated condensing covers are 15°, 30° & 45° and the operational temperature range is from 40^0 to 70^0 at intervals of 5°C. Constant temperature bath was started at 8:30 am an hour before commencing the experimental work to make sure that steady state has been reached. Continuous readings for every half an hour were then taken and recorded under no

fan conditions (natural mode), Table 2 in Appendix 1 shows the readings recorded on 19.06.2012 between 10:00 AM and 03:00 PM. The same process was applied in temperatures 40°C, 45°C, 50°C, 55°C, 60°C, 65°C, 70°C for three inclination angles. Fig. 1 shows the experimental setup and ongoing experiment.

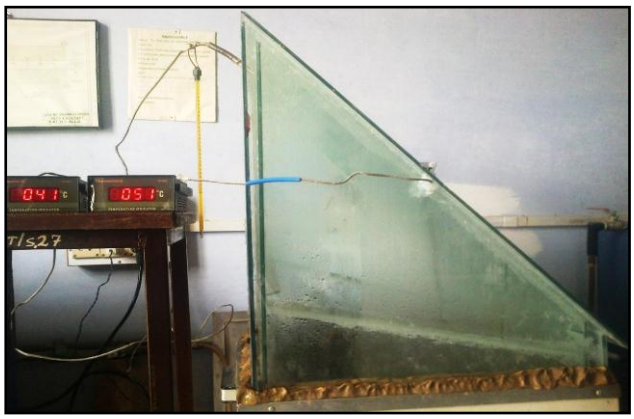

Figure 2: constant temperature water bath with condensing cover during the experiment

3.2 Thermal Model

The vapor, which consists of moisture and dry air, is freely convected above the water surface to the condensing cover by the action of pressure difference because of buoyancy force caused by density variation. This is due to the difference in temperatures between the water surface and condensing cover. This process within the unit always happens in natural mode. However, the external heat transfer from condensing cover to the atmosphere takes place outside the still and can either be under the natural mode, depending on ambient conditions, (Tiwari *et al*, 2005)

3.2.1 Determination of Characteristic Length

It is required to determine the characteristic length for the calculations of internal heat transfer coefficients and convective mass transfer. The Lower vertical height above the water surface is taken as lower characteristic length and higher vertical side as higher characteristic length. So we have taken half of the vertical height at the central axis of condensing cover, this is 120 mm for 15°, 30° & 45°.

Characteristic Length (L_V) = Difference + Vertical Height of smaller end of the solar still (d_f)

Where,
Difference = Height of bath – Height of water

1. 15° = 60 mm + 64 mm = 124 mm = 0.124 m.
2. 30° = 60 mm + 69 mm = 129 mm = 0.129 m.
3. 45° = 60 mm + 75 mm = 135 mm = 0.135 m.

3.2.2 Determination of Temperature Dependent Physical Properties of Vapor

Various temperature dependent physical properties of vapor need to be determined, so as to determine constants C and n. The following expressions are used for the same.

1. Specific heat (C_p)

$$\mathbf{Cp=999.2+0.1434\times T_v+1.101\times 10^{-4}\times T_v^2-6.7581\times 10^{-8}\times T_v^3}$$

2. Density (ρ)

$$\boldsymbol{\rho=\frac{353.44}{(T_v+273.15)}}$$

3. Thermal Conductivity (K_v) $\mathbf{K_v=0.0244+0.7673\times 10^{-4}\times T_v}$

4. Viscosity (μ)
$\mathbf{\mu=1.718\times 10^{-5}+4.620\times 10^{-8}\times T_v}$

5. Latent heat of vaporization of water (L)
when $T_v \leq 70°$ C
$\mathbf{L=2.4935\times 10^6\times\left[1-9.4779\times 10^{-4}T_v+1.3132\times 10^{-7}T_v^2-4.7974\times 10^{-9}T_v^3\right]}$
when $T_v > 70°$ C
$\mathbf{L=3.1615\times 10^6\left[1-\left(7.616\times 10^{-4}\times T_v\right)\right]}$

6. Partial saturated vapor pressure at condensing cover temperature (P_g)

$$\mathbf{P_g=\exp\left[\left(\frac{25.317-5144}{T_g+273}\right)\right]}$$

7. Partial saturated vapor pressure at water temperature (P_w)

$$\mathbf{P_w=\exp\left[\left(\frac{25.317-5144}{T_w+273}\right)\right]}$$

8. Expansion factor (β)

$$\boldsymbol{\beta=\frac{1}{(T_v+273.15)}}$$

3.2.3 Determination of Internal Heat Transfer Coefficients and Convective Mass Transfer

In general for heat transfer the following equations may be applied,

$$\mathbf{Q=h_{cw}\times(T_w-T_g)=h_{cw}\times A\times\Delta T} \quad \text{(eq. 1)}$$

The relation of the non dimensional Nusselt number carries the convective heat transfer coefficient as,

$$\mathbf{Nu=\frac{h_{cw}}{K_v}L_v=C(Gr.Pr)^n} \quad \text{(eq.2)}$$

OR

$$\mathbf{h_{cw}=\frac{K_v}{L_v}C(Gr.Pr)^n} \quad \text{(eq.3)}$$

Where Gr & Pr are given as,

$$\mathbf{Gr=\frac{\beta g L_v^3\rho^2\Delta T}{\mu^2}}$$

$$\mathbf{Pr=\frac{\mu\times C_p}{K_v}}$$

The distillate output in (kg) from the unit can be obtained by the relation,

$$\mathbf{m_{ew}} = \frac{\mathbf{q_{ew} \times A_w \times t}}{\mathbf{L}} \quad \text{(eq.4)}$$

Rate of evaporative heat transfer,

$$\mathbf{q_{ew}} = \mathbf{h_{ew}} \times (\mathbf{T_w} - \mathbf{T_g}) \quad \text{(eq.5)}$$

Evaporative heat transfer coefficient, W/m² °C,

$$\mathbf{h_{ew}} = [(\mathbf{0.01623} \times \mathbf{h_{cw}}) \times \frac{\mathbf{P_w - P_g}}{\mathbf{T_w - T_g}}] \quad \text{(eq.6)}$$

By substituting the expression for h_{cw} from equation (3) into equation (6) we get,

$$\mathbf{h_{ew}} = \mathbf{0.01623} \times \frac{\mathbf{K_v}}{\mathbf{L_v}} \times \mathbf{C} \times (\mathbf{Gr.Pr})^{\mathbf{n}} \times \frac{(\mathbf{P_w - P_g})}{(\mathbf{T_w - T_g})} \quad \text{(eq.7)}$$

Substituting h_{ew} from equation (7) into equation (5) we get,

$$\mathbf{q_{ew}} = \mathbf{0.01623} \times \frac{\mathbf{K_v}}{\mathbf{L_v}} \times \mathbf{C} \times (\mathbf{Gr.Pr})^{\mathbf{n}} \times (\mathbf{P_w - P_g}) \quad \text{(eq.8)}$$

Substituting q_{ew} from equation (8) into equation (4), we get

$$\mathbf{m_{ew}} = \frac{\mathbf{0.01623}}{\mathbf{L}} \times \frac{\mathbf{K_v}}{\mathbf{L_v}} \times \mathbf{A_w} \times \mathbf{t} \times (\mathbf{P_w - P_g}) \times \mathbf{C} \times (\mathbf{Gr.Pr})^{\mathbf{n}} \quad \text{(eq.9)}$$

Equation (9) can be rewritten as,

$$\mathbf{m_{ew}} = \mathbf{R} \times \mathbf{C} \times (\mathbf{Gr.Pr})^{\mathbf{n}}$$

OR

$$\frac{\mathbf{m_{ew}}}{\mathbf{R}} = \mathbf{C} \times (\mathbf{Gr.Pr})^{\mathbf{n}} \quad \text{(eq.10)}$$

Where,

$$\mathbf{R} = \frac{\mathbf{0.01623}}{\mathbf{L}} \times \frac{\mathbf{K_v}}{\mathbf{L_v}} \times \mathbf{A_w} \times \mathbf{t} \times (\mathbf{P_w - P_g}) \quad \text{(eq.11)}$$

Taking the logarithm to both side of equation (10) & comparing it with the straight line equation.

$$\mathbf{y = mx + C} \quad \text{(eq.12)}$$

We get

$$\mathbf{y} = \ln\left(\frac{\mathbf{m_{ew}}}{\mathbf{R}}\right)$$

$$\mathbf{Co} = \ln \mathbf{C}$$

$$\mathbf{X} = \ln\left(\frac{\mathbf{Gr}}{\mathbf{Pr}}\right)$$

$$\mathbf{m = n}$$

By using linear regression analysis the coefficient in equation (12),

$$\mathbf{m} = \frac{\mathbf{N(\Sigma xy) - (\Sigma x)(\Sigma y)}}{\mathbf{(N)(\Sigma x^2) - (\Sigma x)^2}} \quad \text{(eq.13)}$$

$$\mathbf{Co} = \frac{\mathbf{(\Sigma y)(\Sigma x^2) - (\Sigma x)(\Sigma xy)}}{\mathbf{(N)(\Sigma x^2) - (\Sigma x)^2}} \quad \text{(eq.14)}$$

Where,
N = number of experiment observations
C = Exp (Co)
n = m

For the purpose of calculation of the above mentioned work, a computer program was developed in c.net. Table 3 in Appendix 1 shows the different calculated values at 15^O inclination.

4. Result & discussion

It is evident from Fig. 3 and Fig. 4 that vapor temperature and inner glass temperature increases with the decreasing inclination angle. Also it can be seen from Fig. 5 that the temperature difference between evaporative surface and condensing surface increases with increasing inclination angle.

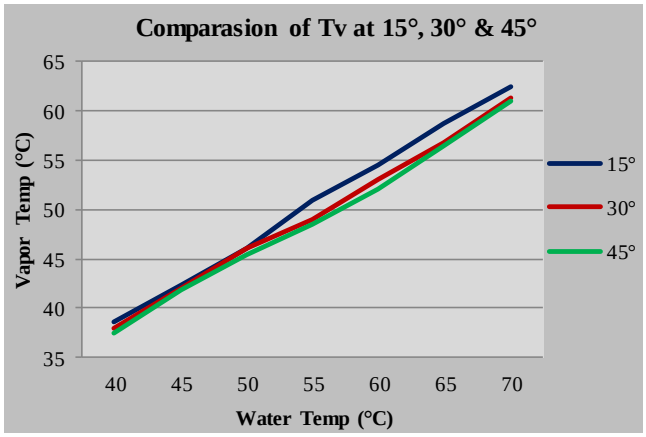

Figure 3: variation of t_v with t_w and inclination angle

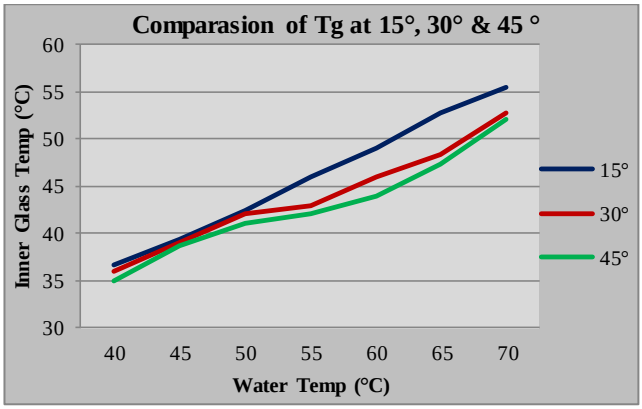

Figure 4: variation of t_g with t_w and inclination angle

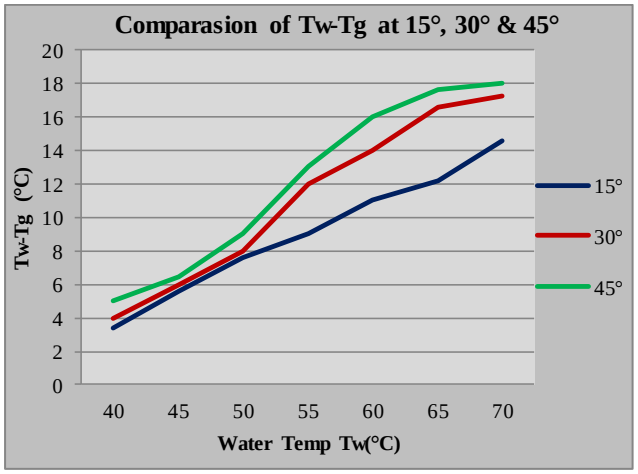

Figure 5: variation of t_w-t_g with t_w and inclination angle

Fig 6, 7 & 8 shows the comparison of convective heat transfer coefficients of present model with Dunkle model. It can be seen that the values of convective heat transfer coefficient for the Present Model are higher than Dunkle model for all three inclinations.

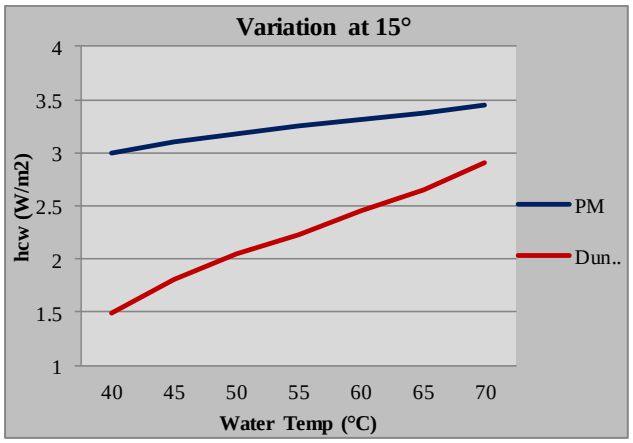

Figure 6: comparison between dunkle and present model at 15° inclination on the basis of h_{cw}

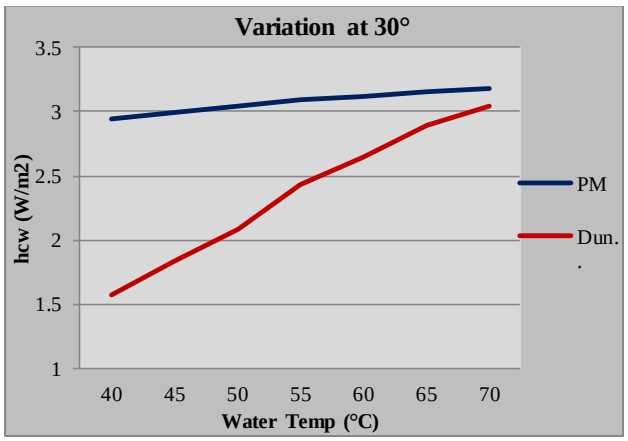

Figure 7: comparison between dunkle and present model at 30° inclination on the basis of h_{cw}

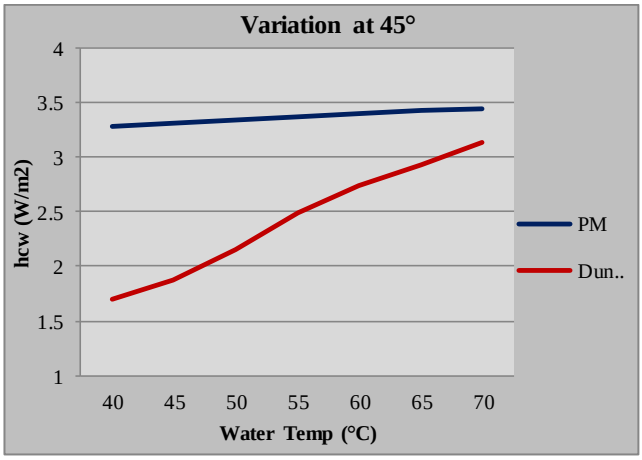

Figure 8: comparison between dunkle and present model at 45° inclination on the basis of h_{cw}

Also Fig 9, 10 & 11 shows the comparison of evaporative heat transfer coefficients of present model with Dunkle model and it can be seen here also that the values of evaporative heat transfer coefficient for the Present Model are higher than Dunkle model for all three inclinations.

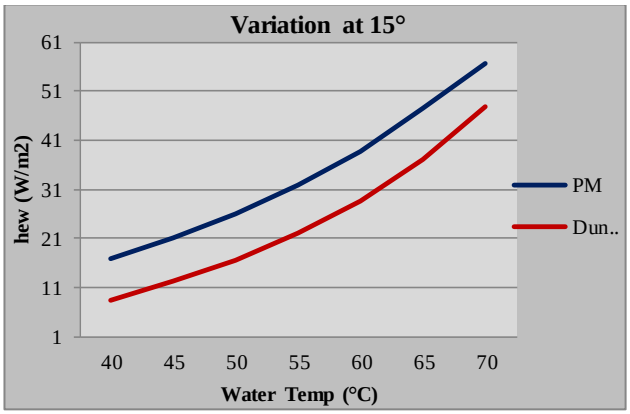

Figure 9: comparison between dunkle and present model at 15° inclination on the basis of h_{ew}

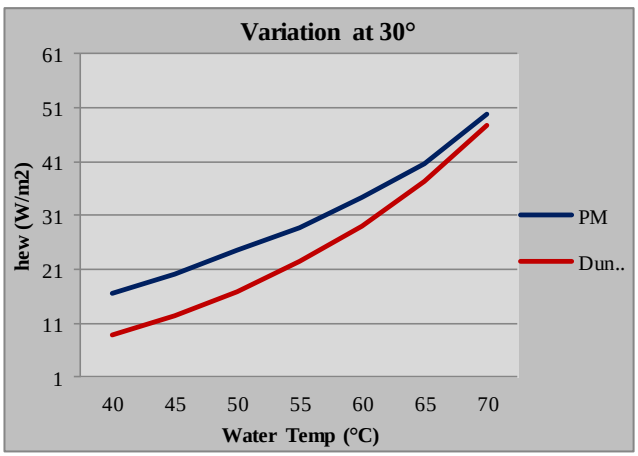

Figure 10: comparison between dunkle and present model at 30° inclination on the basis of h_{ew}

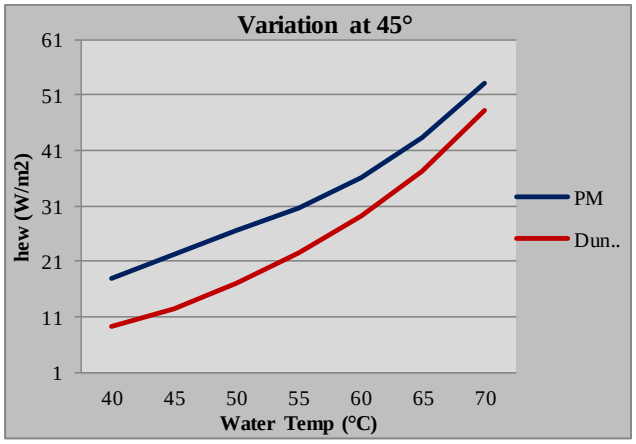

Figure 11: comparison between dunkle and present model at 45° inclination on the basis of h_{ew}

Fig. 12 and Fig. 13 shows the variation of convective heat transfer coefficient and evaporative heat transfer coefficient with water temperature and inclination angle. It can be observed that the maximum convective heat transfer coefficient is for 45^{O} inclination angle and the minimum is for 30^{O} inclination angle. Also maximum evaporative heat transfer coefficient is for 15^{O} inclination angle and the minimum is for 30^{O} inclination angle. Both convective and evaporative heat transfer coefficients increase with increase in water temperature.

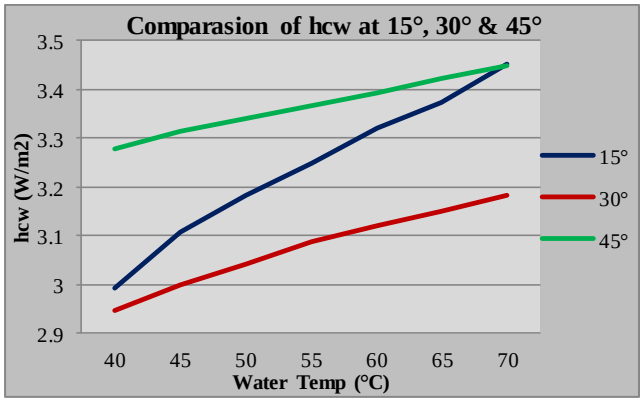

Figure 12: variation of h_{cw} with inclination angles and t_w

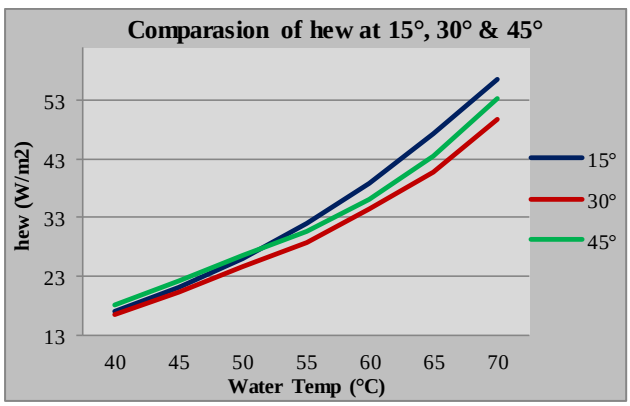

Figure 13: variation of h_{ew} with inclination angles and t_w

Fig.14 gives comparison between Dunkle Distillate output (m_{ewD}), theoretical distillate output (m_{ewT}) and measured distillate output (m_{ew}) for 15° inclination of at different water temperature. It is clearly seen that the values of distillate output of Present Model are higher than the values of Dunkle Model.

As the difference between the theoretical values and present model values is not much that means the present model is working properly to give distillate output. The maximum and minimum % deviation between the theoretical and practical is 11.46% for 70° C & -3.42% for 45° C respectively.

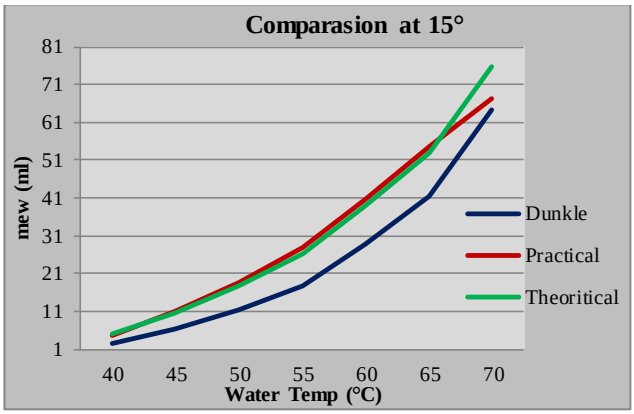

Figure 14: comparasion between present, dunkle and theoritical model on the basis of m_{ew} at 15° inclination

Fig.15 gives comparison between Dunkle Distillate output (m_{ewD}), theoretical distillate output (m_{ewT}) and measured distillate output (m_{ew}) at different water temperature for 30° inclination angle. It is clearly seen that the values of distillate output of Present Model are higher than the values of Dunkle Model. The maximum and minimum % deviation between the theoretical and practical is -04.71% for 70° C & -1.36% for 60° C respectively.

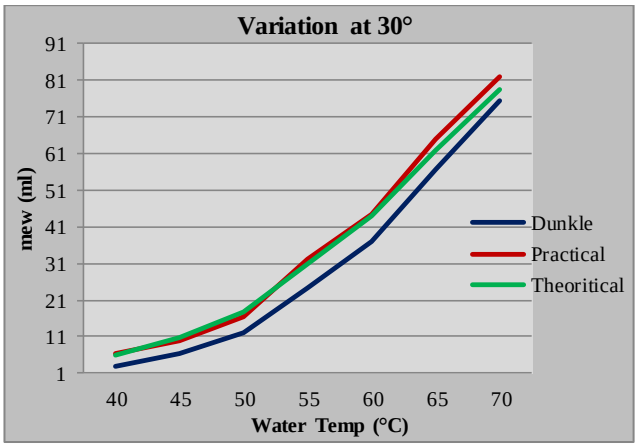

Figure 15: comparasion between present, dunkle and theoritical model on the basis of m_{ew} at 30° inclination

Fig.16 gives comparison between Dunkle Distillate output (m_{ewD}), theoretical distillate output (m_{ewT}) and measured

distillate output (m_{ew}) at different water temperature for 45° inclination angle. It is clearly seen that the values of distillate output of Present Model are higher than the values of Dunkle Model. The maximum and minimum % deviation between the theoretical and practical is -10.52% for 70° C & -1.96% for 45° C respectively.

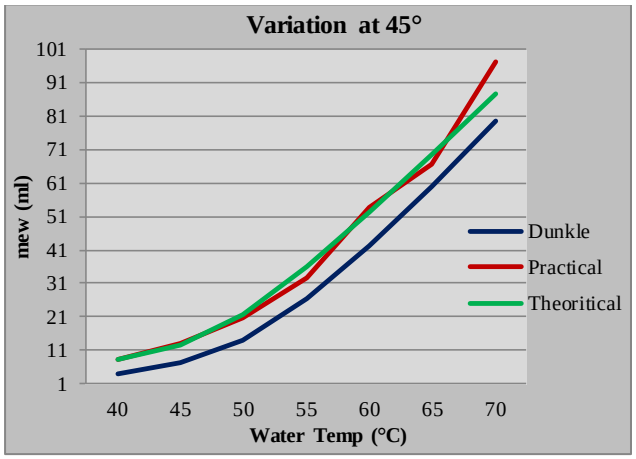

Figure 16: comparasion between present, dunkle and theoritical model on the basis of m_{ew} at 45° inclination

Fig 17 it can be clearly seen that the yield increases as the inclination angle of the condensing cover increases and the water, vapor and inner glass temperature decreases.
It is because of the fact that yield is the product of heat transfer coefficient and ΔT and is greatly influenced by ΔT. The is yield is maximum for condensing cover with the inclination angle of 45° and is minimum for the condensing cover with the inclination angle of 15°. This is because of the fact that ΔT increases with increase in inclination angle of the condensing cover.

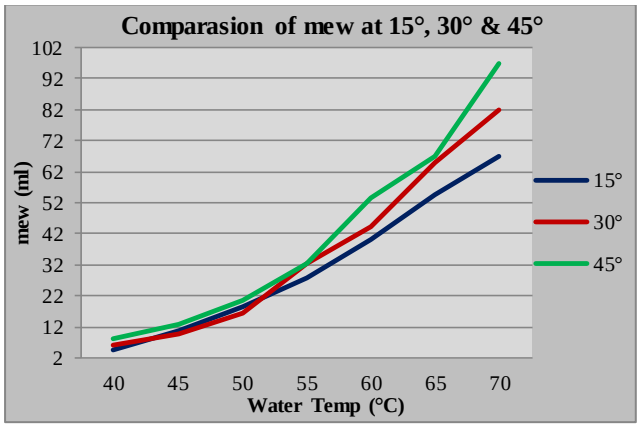

Figure 17: variation of m_{ew} with inclination angles and t_w

Conclusions

Following conclusions can be drawn from this study.

1. Convective and Evaporative heat transfer coefficients of condensing covers inclined at 15^0, 30^0 & 45^0 are higher than Dunkle model.
2. Distillate output of condensing covers inclined at 15^0, 30^0 & 45^0 is higher than Dunkle model.
3. The maximum yield is obtained for condensing cover with the inclination angle of 45° and the minimum is obtained for the condensing cover with the inclination angle of 15°.
4. The temperature difference between evaporative surface and condensing surface increase with increase in inclination angel and water temperature.
5. Distillate output increases with increase in temperature difference between evaporating surface and condensing surface and with increase in inclination angle.

References

Tiwari GN (2002) Solar Energy. *Narosa Publishing* House. New Delhi

Dunkle, R.V.(1961), Solar water distillation: The roof type still and multiple effect diffusion still, International Development in Heat Transfer, ASME, Proceedings of International Heat Transfer, Part v, *University of Colorado*, pp.895.

Nafey AS, Abdelkader M, AbdelmotalipA,Mabrouk AA (2000) Parameters affecting solar still productivity. Energy Convers Manage 41(16):1797–1809.

Akash BA, Mohsen MS, Nayfeh W (2000) Experimental study of the basin type solar still under local climate conditions. *Energy Convers Manage* 41(9): pp. 883–890.

Kumar, Sanjay and Tiwari, G.N. (1996), Estimation of Convective Mass Transfer in Solar Distillation System, *Solar Energy*, pp. 457-459.

Lof G.O.G., Eibling, J.A., Blomer, J.W. (1961), Energy Balances in Solar Distillation, *J. Am. Inst. Chem. Eng*. 7, 4, pp. 641.

Sharma V.B. and Mullick S.C. (1991), Estimation of heat transfer coefficients, the upward heat flow and evaporation in a solar still, *Transaction of the ASME* 113, pp. 36-43.

Shukla S.K. and Sorayan V.P.S. (2005), Thermal modelling of solar stills: An experimental validation, *Renewable Energy*, 30, pp 683-699.

Aboul-Enein S, El-Sebaii AA, El-Bialy E (1998) Investigation of a single-basin solar still with deep basins. *Renew Energy14* (1–4):299–305.

Akash BA, Mohsen MS, Osta O, Elayan Y (1998) Experimental evaluation of a Single-basin solar still using different absorbing materials. *Renew Energy* 14(1–4):307–310

Tiwari Anil Kr., Tiwari G. N. (2005), Effect of the condensing cover's slope on Internal heat and mass transfer in distillation: an Indoor Simulation, *Elsevier publication*. *Desalination* pp 73-88.

Sampathkumar K, Arjunan T.V., Pitchandi P., and Senthilkumar P., (2010), 'Active solar distillation—A detailed review', *Renewable and Sustainable Energy Reviews* Vol-14, pp. 1503–1526.

Delyannis E, (2003), 'Historic background of desalination and renewable energies', *Solar Energy*, 75, PP.357–366

Table 2: Experimental data record for condensing cover at an inclination of 15°

S. No	Time (t) = 30 min	Water Temp (°C)	Vapor Temp (°C)	Inner glass Temp (°C)	Condensate Output (ml)
1.	10:00	29	31	33	Nil
2.	10:30	40	38	36	Nil
3.	11:00	40	38	36	Nil
4.	11:30	40	38	36	Nil
5.	12:00	40	38	36	Nil
6.	12:30	40	38	36	Nil
7.	01:00	40	38	36	4
8.	01:30	40	38	36	6
9.	2:00	40	39	37	5
10.	02:30	40	39	37	5
11.	03:00	40	39	37	4
	Avg.	40	193/5 = 38.6	183/5 = 36.6	24/5 = 4.8

Table 3: Calculated values for inclination angle of 15°

T_w	1 (40°C)	2 (45°C)	3 (50°C)	4 (55°C)	5 (60°C)	6 (65°C)	7 (70°C)
T_v	38.6	42.4	46	51	53.8	58.8	62.4
Tg	36.6	39.4	42.4	46.0	47.8	52.8	55.4
L_v	0.12	0.12	0.12	0.12	0.12	0.12	0.12
m_{ew}	0.0048	0.011	0.0184	0.028	0.0404	0.054	0.0672
L	2411230.019	2402080.385	2393412.31	2381373.318	2372223.684	2362592.491	2351516.618
K_v	0.0483	0.04860	0.0488	0.0492	0.0495	0.0498	0.0502
β	0.00320	0.003170	0.003134	0.0030864	0.003050	0.0030137	0.002972
ρ	1.1342	1.1206	1.1079	1.0908	1.0782	1.0652	1.0506
ΔT	4.8229	8.4768	12.4015	16.0639	21.5774	26.7844	35.8203
P_w	7204.745	9329.151	11983.708	15276.533	19332.686	24295.9534	30330.69309
P_{ci}	6015.007	6980.884	8164.507	9814.421	11405.428	13741.455	15571.1542
R	0.0006962	0.0013879	0.0022749	0.0032967	0.0048324	0.006499	0.009168
Gr	338195.1865	566826.9488	793230.6992	966619.5193	1239528.116	1467649.633	1858645.333
Pr	0.68806	0.6881	0.68932	0.68930	0.68935	0.68962	0.6892
μ	3.1575E-05	3.1751E-05	3.1917E-05	3.2148E-05	3.2324E-05	3.2509E-05	3.2720E-05
C_p	1052.528	1053.26404	1053.954	1054.920	1055.656	1056.4325	1057.5283
X	12.3574	12.8740	13.2118	13.4094	13.6582	13.8275	14.0632
Y	1.9307	2.0701	2.0904	2.1392	2.1234	2.1254	1.9919
XY	23.8584	26.6504	27.6179	28.6853	29.0018	29.3889	28.0124
X^2	152.7053	165.7398	174.5516	179.8120	186.5464	191.1997	197.7735

Abbreviations

A Area, m^2
C Constant
C_p Specific heat of working fluid, J/kg°C
d_f Vertical height of the smaller end of the still, m
g Acceleration due to gravity, m/s^2
Gr Grashof number
h_{ew} Evaporative heat transfer coefficient, W/m^2
h_{cw} Convective heat transfer coefficient W/m^2
L Latent heat of vaporization, J/kg
L_v Characteristic Length, m
M Initial mass of water (kg)
m_{ew} Mass of distillate output (kg)
n Constant
P_w Partial vapor pressure at water temp., N/m^2
P_g Partial vapor pressure at glass temp., N/m^2
Pr Prandtl Number
T_a Ambient temperature (°C)
T_g Glass temperature (°C)
T_w Water temperature (°C)
T_v Vapor temperature (°C)

Special Characters

μ Dynamic Viscosity of fluid, $N.s/m^2$
ρ Density of humid air, kg/m^3
ΔT Effective temperature difference (°C)